PHYSICAL REVIEW B VOLUME 10, NUMBER 6 15 SEPTEMBER 1974

Inelastic scattering of low-energy electrons from a crystal surface

Masakuzu Ichikawa*
Department of Physics, School of Science and Engineering, Waseda University, Tokyo, Japan
(Received 2 October 1973)

The inelastic-scattering probability of low-energy electrons due to the bulk- and surface-plasmon excitations is calculated using the infinite-square-barrier model. When the dispersion of the plasmons is neglected, the probability becomes the one derived by using the high-frequency step-density model. In order to consider the scattering by the lattices and the absorption effects for an incident electron, the distorted-wave method is used, which upon some manipulation gives essentially the same inelastic intensities as the ones given by Duke and Laramore. Some numerical calculations are performed for the Al(111) surface, and it is found that the absorption plays an important role in determining the intensity for the bulk plasmon relative to the one for the surface plasmon, and the cutoff wave numer at $k = 0$ has some influence on the angular profile. The intensities obtained in this paper are qualitatively in agreement with the experimental results.

I. INTRODUCTION

With the recent development of the low-energy-electron-diffraction (LEED) apparatus, many experimental studies[1–5] which investigate inelastically scattered waves from the crystal surface with the characteristic energy losses have been performed in order to determine the properties of the electrons inside the crystal. Many theoretical studies[6–11] on the elementary excitations—especially the surface plasmon, created in the electron gas bounded by surface potential—have appeared, and recently the detailed dispersion relations for the surface plasmon have been obtained using microscopic theory.[12–14] The theoretical studies are mainly concerned with the dispersion relations for the surface plasmon, but in order to compare the theoretical results with the experimental ones by LEED, it is important and necessary to consider the effects of diffraction and absorption which are caused by strong interactions with the crystal. The qualitative treatment considering the above effects was discussed by several authors,[15–17] but the quantative and detailed treatment was first discussed by Duke and Laramore.[18] They proposed a quantum-field-theoretical method using a model Hamiltonian for surface and bulk plasmons, where the effects of diffraction and absorption were taken into consideration. Recently they have made detailed comparisons with the experimental results to obtain the dispersion relation for the surface plasmon.[19–25] In the comparison with experimental results, they used dispersion-dependent cutoff values at $k = 0$ in order to avoid the unphysical divergence. However, it is found in later discussions that the cutoff value is rather independent of the dispersion, and the variations of the cutoff value have some influence on the angular profile and magnitudes of the inelastic intensities. In our opinion, it is therefore necessary to consider inelastic scattering from a different point of view.

We use the infinite-square-barrier model[6,9] to investigate the interaction of the incident electron with the electrons inside the crystal. In the case of small wave number $k \ll k_c$, the scattering probability obtained by this model can be represented by the dielectric function, which is useful for considering the problem of the cutoff value, and if we take into account only the collective excitations and neglect the dispersion relations, we obtain the same scattering probability as the one given by the high-frequency step-density model.[26,27] Then the model used here makes possible general considerations of the scattering probability.

On the other hand, we use the distorted-wave method to consider the effects of diffraction and absorption on the inelastic intensities, where only the waves coherent with the nonscattered waves are taken. When we use any relations, the results become essentially the same as the ones of Duke and co-workers,[18,23] and we can easily consider the dynamical effect due to the strong interaction with the atoms by using the dynamical wave functions for the incident electrons. Thus it is considered useful to investigate inelastic scattering by the above treatment.

In Sec. II the general treatment of the inelastic scattering probability is presented. In Sec. III we calculate the intensities from the Al(111) surface using the formula derived in Sec. II and compare the theoretical results with the experimental ones.

II. THEORY OF INELASTIC SCATTERING PROBABILITY

A. General treatment of inelastic scattering probability

We consider a system where an incident electron is inelastically scattered due to the electrons inside the crystal and elastically scattered by the crystal lattices. Here the system for the electrons in the

crystal is supposed to be homogeneous parallel to the crystal surface, since only the collective excitations are concerned and the corrections due to the imhomogeneity are considered to be small. If we take the first Born approximation with respect to the interaction of the incident electron with the electron gas in the crystal, the total scattering probability of the incident electron is given by

$$\sigma=\frac{1}{4\pi^3 v\hbar}\sum_{\vec{k}}\int d\vec{K}'\int d\vec{r}\int d\vec{r}'\varphi_{\vec{K}'}^{(-)*}(\vec{r}')\varphi_{\vec{K}}^{(-)}(\vec{r})\,e^{i\vec{k}\cdot(\vec{X}-\vec{X}')}\times\varphi_{\vec{K}}^{(+)*}(\vec{r})\,\varphi_{\vec{K}'}^{(+)}(\vec{r}')S(\vec{k},\omega,z,z') \quad , \tag{2.1}$$

$$S(\vec{k},\omega,z,z')=-\operatorname{Im}\int dz_1\int dz_2\, v(k,z-z_1)\times P(\vec{k},\omega,z_1,z_2)v(k,z_2-z') \quad , \tag{2.2}$$

$$\omega=\frac{\hbar K^2}{2m}-\frac{\hbar K'^2}{2m}+i\epsilon, \quad \vec{r}=(\vec{X},z),$$

$$v(k,z_2-z_1)=\frac{2\pi e^2 e^{-k|z_2-z_1|}}{k} \quad .$$

In the above, $\hbar^2K^2/2m$ and $\hbar^2K'^2/2m$ are the initial and the final energies for the incident electron, respectively. $v(k,z-z')$ is the Fourier component of the Coulomb potential parallel to the crystal surface, and v is the velocity of the incident electron. $\varphi_{\vec{K}}^{(+)}(\vec{r})$ and $\varphi_{\vec{K}'}^{(-)}(\vec{r})$ are the initial and final wave functions for the incident electron, respectively, and are discussed later in detail. $P(\vec{k},\omega,z,z')$ is the Fourier component of the density correlation function parallel to the surface, and in the random-phase approximation it satisfies

$$P(\vec{k},\omega,z_1,z_2)=P_0(\vec{k},\omega,z_1,z_2)+\int dz_3\int dz_4\,P_0(\vec{k},\omega,z_1,z_3)\,v(k,z_3-z_4)\,P(\vec{k},\omega,z_4,z_2) \quad , \tag{2.3}$$

$$P_0(\vec{k},\omega,z_1,z_2)\equiv\frac{-2}{\hbar(2\pi)^2}\int d\vec{q}\sum_{n,n'}\frac{\theta(\omega_{\vec{q},n}-\omega_F)-\theta(\omega_{\vec{k}+\vec{q},n'}-\omega_F)}{\omega+\omega_{\vec{k},n}-\omega_{\vec{k}+\vec{q},n'}}\varphi_n^*(z_1)\varphi_{n'}(z_1)\varphi_{n'}^*(z_2)\varphi_n(z_2) \quad , \tag{2.4}$$

where $\varphi_n(z)e^{i\vec{k}\cdot\vec{X}}$ is the single-particle wave function for the electron in the crystal, $\hbar\omega_{\vec{k},n}\equiv\hbar^2k^2/2m+E_n$, and E_n is the energy associated with wave function $\varphi_n(z)$. $\hbar\omega_F$ is the Fermi energy and $\theta(t)$ the step function.

In order to solve the integral Eq. (2.3), we use a model where the electrons in the crystal are bounded by infinite-square-potential walls at $z=0$ and $z=l$.[9,10,13] As the electrons cannot penetrate the potentials, we take $\varphi_n(z)=1/\sqrt{l}\sin n\pi/l_z$ where n is a positive integer and the density correlation function does not vanish only in $0\le z\le 1$. So the functions in Eqs. (2.3) and (2.4) can be represented by the Fourier series as

$$f(\vec{k},z,z')=\sum_{p_n>0}\sum_{p_{n'}>0}f(\vec{k},p_n,p_{n'})\cos(p_nz)\cos(p_{n'}z'), \qquad p_n=\frac{(2n+1)\pi}{l} \quad , \quad p_{n'}=\frac{(2n'+1)\pi}{l} \quad . \tag{2.5}$$

In Eq. (2.5) we confine ourselves to odd momentum $(2n+1)\pi/l$, since the choice of the momentum becomes less important when $l\to\infty$. Introducing the Fourier representation by using Eq. (2.5) and after some calculations (in the following discussions we take $kl\to\infty$) we get from Eq. (2.3)

$$P(\vec{k},\omega,z,z')=\sum_{p_{n_1}}\sum_{p_{n_2}>0}\frac{k^2+p_{n_2}^2}{\pi e^2 l}[(1-D)^{-1}(\vec{k},\omega,p_{n_1},p_{n_2})-\delta_{p_{n_1},p_{n_2}}]\cos(p_{n_1}z)\cos(p_{n_2}z')$$
$$-\frac{2k}{\pi e^2 l}\sum_{p_{n_1}}\sum_{p_{n_3}>0}[(1-D)^{-1}(\vec{k},\omega,p_{n_1},p_{n_3})-\delta_{p_{n_2},p_{n_3}}]\cos(p_{n_1}z)\sum_{p_{n_4}}\sum_{p_{n_2}>0}[(1-D)^{-1}(\vec{k},\omega,p_{n_2},p_{n_4})-\delta_{p_{n_4},p_{n_2}}]$$
$$\times\cos(p_{n_2},z')\Big/\Big(1+\frac{2k}{l}\sum_{p_{n_3}}\sum_{p_{n_4}>0}\frac{1}{k^2+p_{n_4}^2}[(1-D)^{-1}(\vec{k},\omega,p_{n_3},p_{n_4})-\delta_{p_{n_3},p_{n_4}}]\Big) \quad , \tag{2.6}$$

where the function $(1-D)^{-1}(\vec{k},\omega,p_{n_1},p_{n_2})$ is defined by

$$\sum_{p_{n_3}>0}(1-D)^{-1}(\vec{k},\omega,p_{n_1},p_{n_3})[\delta_{p_{n_3},p_{n_2}}-D(\vec{k},\omega,p_{n_3},p_{n_2})]=\delta_{p_{n_1},p_{n_2}} \quad , \tag{2.7a}$$

$$D(\vec{k},\omega,p_{n_1},p_{n_2})=\frac{e^2}{(k^2+p_{n_2}^2)\pi l\hbar}\Big[\sum_{p_m=-\infty}^{\infty}F(\vec{k},\omega,p_m,p_m+p_{n_1})\,\delta_{p_{n_1},p_{n_2}}-F\Big(\vec{k},\omega,\frac{p_{n_1}-p_{n_2}}{2},\frac{p_{n_1}+p_{n_2}}{2}\Big)$$
$$-F\Big(\vec{k},\omega,\frac{p_{n_1}+p_{n_2}}{2},\frac{p_{n_1}-p_{n_2}}{2}\Big)\Big], \tag{2.7b}$$

$$F(\vec{k},\omega,p_m,p_{m'})=\int d\vec{q}\,\frac{-\theta(\omega_{\vec{q},m}-\omega_F)+\theta(\omega_{\vec{q}+\vec{k},m'}-\omega_F)}{\omega+\omega_{\vec{k},m}-\omega_{\vec{k}+\vec{q},m'}}\,, \tag{2.7c}$$

where $p_m=m\pi/l$, m is an integer. In Eq. (2.6) we multiplied the result by a factor of 2, because we must consider the density correlation function in the case of even momentum $2n\pi/l$.

The second term in Eq. (2.6) shows the surface effects and its pole gives the surface-plasmon dispersion relation, which is the same result given by several authors.[9,10,12,13] Combining Eq. (2.6) with Eqs. (2.1) and (2.2) we may obtain the exact scattering probability, but owing to the complicated structure of Eq. (2.7b) it is practically impossible to use the result in Eq. (2.6) to calculate the scattering probability. Fortunately, however, we may neglect off-diagonal terms in Eq. (2.7b) in the case of small wave number[10,13]; $k\ll k_c$ (k_c is the plasmon cutoff wave number), in which we are interested in the following discussion. Then Eq. (2.6) is rewritten as

$$P(\vec{k},\omega,z,z')=\sum_{p_{n_1}>0}\frac{k^2+p_{n_1}^2}{\pi e^2 l}\,\frac{1-\epsilon(\vec{k},\omega,p_{n_1})}{\epsilon(\vec{k},\omega,p_{n_1})}\cos(p_{n_1}z)\cos(p_{n_2}z')-\frac{2k}{\pi e^2 l^2}\sum_{p_{n_1}>0}\frac{1-\epsilon(\vec{k},\omega,p_{n_1})}{\epsilon(\vec{k},\omega,p_{n_1})}\cos(p_{n_1}z)$$
$$\times\sum_{p_{n_2}>0}\frac{1-\epsilon(\vec{k},\omega,p_{n_2})}{\epsilon(\vec{k},\omega,p_{n_2})}\cos(p_{n_2}z')\Big/\left(1+\frac{2k}{l}\sum_{p_{n_3}>0}\frac{1}{k^2+p_{n_3}^2}\,\frac{1-\epsilon(\vec{k},\omega,p_{n_3})}{\epsilon(\vec{k},\omega,p_{n_3})}\right)\,, \tag{2.8}$$

where $\epsilon(\vec{k},\omega,p_n)$ is the dielectric function of Lindhard. The result of Eq. (2.8) is familiar and is useful for calculating the inelastic intensities due to the electronic excitation, especially due to the plasmon excitations, which are important in investigating the surface properties of the crystal by LEED. In Sec. II B and C we consider only the plasmon excitations.

B. Bulk-plasmon excitation

Here we calculate the scattering probability due to the bulk-plasmon excitation. Substituting Eq. (2.8) into Eq. (2.2) and using the relation when $kl\to\infty$ we have

$$\int_0^l\cos(p_n z_1)\frac{e^{-k|z-z_1|}}{k}\,dz_1=\frac{e^{kz}}{k^2+p_n^2}\qquad(z<0)$$
$$=\frac{2\cos(p_n z)-e^{-kz}}{k^2+p_n^2}\qquad(z>0)\,. \tag{2.9}$$

The spectral functions $S(\vec{k},\omega,z,z')$ is obtained as follows:

(i) $z<0$ *and* $z'<0$

$$S(\vec{k},\omega,z,z')=-\operatorname{Im}e^{kz}e^{kz'}2e^2\int_0^\infty dp\,\frac{1}{k^2+p^2}\,\frac{1-\epsilon(\vec{k},\omega,p)}{\epsilon(\vec{k},\omega,p)}\Big/\left(1+\frac{k}{\pi}\int_0^\infty dp\,\frac{1-\epsilon(\vec{k},\omega,p)}{\epsilon(\vec{k},\omega,p)}\right)\,, \tag{2.10a}$$

where we use the relation

$$\sum_{p_n>0}\to\frac{l}{2\pi}\int_0^\infty dp\,.$$

(ii) $z<0$ *and* $z'>0$

$$S(\vec{k},\omega,z,z')=-\operatorname{Im}2e^2e^{kz}\int_0^\infty dp\,\frac{1-\epsilon(\vec{k},\omega,p)}{\epsilon(\vec{k},\omega,p)}\,\frac{2\cos(pz)-e^{-kz}}{k^2+p^2}\Big/\left(1+\frac{k}{\pi}\int_0^\infty dp\,\frac{1-\epsilon(\vec{k},\omega,p)}{\epsilon(\vec{k},\omega,p)}\right)\,. \tag{2.10b}$$

(iii) $z>0$ *and* $z'<0$

The result is obtained by interchanging z and z' in Eq. (2.10b).

(iv) $z>0$ *and* $z>0$

$$S(\vec{k},\omega,z,z')=-\operatorname{Im}\Big[2e^2\int_0^\infty dp\,\frac{1-\epsilon(\vec{k},\omega,p)}{\epsilon(\vec{k},\omega,p)}\,\frac{[2\cos(pz)-e^{-kz}][2\cos(pz')-e^{-kz'}]}{k^2+p^2}$$
$$-\frac{2e^2}{\pi}k\int_0^\infty dp\,\frac{1-\epsilon(\vec{k},\omega,p)}{\epsilon(\vec{k},\omega,p)}\,\frac{[2\cos(pz)-e^{-kz}]}{k^2+p^2}$$

$$\times\int_0^\infty dp'\frac{1-\epsilon(\vec{k},\omega,p')}{\epsilon(\vec{k},\omega,p')}\frac{[2\cos(p'z')-e^{-kz'}]}{k^2+p'^2}\Big/\left(1+\frac{k}{\pi}\int_0^\infty dp'\frac{1}{k^2+p'^2}\frac{1-\epsilon(\vec{k},\omega,p')}{\epsilon(\vec{k},\omega,p')}\right)\Big] \quad . \tag{2.10c}$$

At first we investigate cases (i)–(iii). Here we consider only the case of small wave number $k \ll k_c$. The main term of the spectral function originates from the pole of $1/(k^2+p^2)$, because it gives a term proportional to $1/k$. Then the spectral function in this region is given approximately by

$$S(\vec{k},\omega,z,z') = -\operatorname{Im}\frac{2\pi e^2}{k}e^{-k|z|}e^{-k|z'|}\frac{1-\epsilon(\omega)}{1+\epsilon(\omega)} , \tag{2.11}$$

where $\epsilon(\omega)=1-\omega_p^2/\omega^2$. From Eq. (2.11) it is clear that in the case $k \ll k_c$ the spectral function for the bulk plasmon is zero outside the crystal and only the one for the surface-plasmon excitation is nonzero. Next we will investigate the case of $z>0$ and $z'>0$. In order to get a more useful result, we must make further approximations of the second term in Eq. (2.10c). At first we take

$$\int_0^\infty dp\frac{1-\epsilon(\vec{k},\omega,p)}{\epsilon(\vec{k},\omega,p)}\frac{[2\cos(pz)-e^{-kz}]}{k^2+p^2} \approx \int_0^\infty dp\frac{1-\epsilon(\vec{k},\omega,p)}{\epsilon(\vec{k},\omega,p)}\frac{e^{-kz}}{k^2+p^2} , \tag{2.12}$$

which may be a good approximation in the case $k \ll k_c$, because the main contribution to the above value is due to the pole of $1/(k^2+p^2)$, and the relation in Eq. (2.12) is exactly correct when the dispersion of $\epsilon(\vec{k},\omega,p)$ is neglected. Since we consider the bulk-plasmon excitation, which means $\epsilon(\vec{k},\omega,p)\approx 0$, the factor 1 in the denominator may be neglected compared with the second term,

$$\frac{k}{\pi}\int_0^\infty dp\frac{1}{k^2+p^2}\frac{1-\epsilon(\vec{k},\omega,p)}{\epsilon(\vec{k},\omega,p)} .$$

Then the terms

$$\int_0^\infty dp\frac{1}{k^2+p^2}\frac{1-\epsilon(\vec{k},\omega,p)}{\epsilon(\vec{k},\omega,p)}$$

in both the numerator and denominator cancel each other, and finally we obtain the spectral function for the bulk plasmon in the case $z\geq 0$ and $z'\geq 0$:

$$S(\vec{k},\omega,z,z') = -\operatorname{Im}4e^2\int_0^\infty\frac{1-\epsilon(\vec{k},\omega,p)}{\epsilon(\vec{k},\omega,p)}\frac{1}{k^2+p^2} \times[2\cos(pz)\cos(pz')-\cos(pz)e^{-kz'} - e^{-kz}\cos(pz')] . \tag{2.13}$$

If we neglect the dispersion of $\epsilon(\vec{k},p,\omega)$, which is valid when small wave number $k\approx 0$ is concerned and the density of the electrons is high, Eq. (2.13) may be rewritten as

$$S(\vec{k},\omega,z,z') = -\frac{2\pi e^2}{k}\operatorname{Im}\frac{\omega_p^2}{\omega^2-\omega_p^2}(e^{-k|z-z'|}-e^{-k(z+z')}) , \tag{2.14}$$

which is exactly the same result given by the high-frequency step-density model where the conservation law between the modes for the bulk plasmon and those for the surface plasmon is precisely considered[26] (see Appendix B).

In order to consider the damping of the bulk plasmon in the region $k<k_c$, we may replace the dielectric function in Eq. (2.13) by the generalized dielectric function which examines the interband transition,[28] since the local field correction to the plasmon field may be considered to be small. Then from Eqs. (2.13) and (2.1) we obtain the scattering probability due to the bulk-plasmon excitation,

$$\sigma_b=\frac{e^2\omega_p}{4\pi^3 v}\int d\vec{K}'\int_0^{p_c}dp \times\sum_{\vec{k}}\frac{1}{k^2+p^2}\frac{\hbar\Gamma_b(k,p)}{[\hbar\omega-\hbar\omega_b(k,p)]^2+[\hbar\Gamma_b(k,p)]^2} \times\{|\langle\varphi_{\vec{K}'}^{(-)}|\theta(z)[2\cos(pz)-e^{-kz}]e^{-i\vec{k}\cdot\vec{x}}|\varphi_{\vec{K}}^{(+)}\rangle|^2 - |\langle\varphi_{\vec{K}'}^{(-)}|\theta(z)e^{-kz}e^{-i\vec{k}\cdot\vec{x}}|\varphi_{\vec{K}}^{(+)}\rangle|^2\} , \tag{2.15}$$

where $\Gamma_b(k,p)$ and $\hbar\omega_b(k,p)$ are the momentum-dependent damping frequency and the excitation energy, respectively, for the bulk plasmon and p_c is the plasmon cutoff value. When we fix the parallel momentum k in Eq. (2.15), the result in Eq. (2.15) seems to have a divergence like $1/k$ near $k\approx 0$, which originates from the poles of $1/(k^2+p^2)$ in the integration with respect to the perpendicular momentum p. This is not the case however, since from the form of Eq. (2.14) one can see that the spectral function is finite at $k=0$. So we think the formula in Eq. (2.15) gives a good approximation for the bulk-plasmon excitation in the region $k \ll k_c$.

C. Surface-plasmon excitation

The spectral function for the surface plasmon is obtained from the second term in Eq. (2.6), whose denominator gives the surface-plasmon excitation energy. The term $\sum_{p_{n_1}}\sum_{p_{n_3}}[(1-D)^{-1}(\vec{k},\omega, p_{n_1},p_{n_3})-\delta_{p_{n_1},p_{n_3}}]\cos(p_{n_1}z)$ at $\omega=(\omega_p/\sqrt{2})$ in the numerator is proportional to the induced charge-density fluctuation, which vanishes at the surface $z=0$, and the potential field for the surface plasmon is obtained from this charge fluctuation. In the case $k \ll k_c$ we may neglect the off-diagonal parts in Eq. (2.7b).[10] That means the charge fluctuation is nonzero at the surface, but the potential field obtained in this approximation may be a good

one because we notice only the long-range part of the interaction in $k \ll k_c$, which is insensitive to the details of the charge fluctuation near the surface. Then we can obtain the spectral function for the surface plasmon from the second term in Eq. (2.8), since the first term may be negligible near $\omega \approx (\omega_p/\sqrt{2})$,

$$S(\vec{k},\omega,z,z') = \mathrm{Im}\frac{2e^2}{\pi} k \int_0^l dz_1 \int_0^\infty dp \frac{1-\epsilon[\vec{k},(\omega_p/\sqrt{2}),p]}{\epsilon[\vec{k},(\omega_p/\sqrt{2}),p]} \cos(pz_1) \frac{e^{-k|z-z_1|}}{k} \int_0^l dz_2 \int_0^\infty dp \frac{1-\epsilon[\vec{k},(\omega_p/\sqrt{2}),p]}{\epsilon[\vec{k},(\omega_p/\sqrt{2}),p]} \times \cos(pz_2) \frac{e^{-k|z'-z_2|}}{k} \Big/ \left(1+\frac{k}{\pi}\int_0^\infty dp \frac{1}{k^2+p^2} \frac{1-\epsilon(\vec{k},\omega,p)}{\epsilon(\vec{k},\omega,p)}\right) . \quad (2.16)$$

Now we investigate the potential part in Eq. (2.16). When we take the dielectric function $\epsilon[\vec{k},(\omega_p/\sqrt{2}),p]$

$$\epsilon[\vec{k},(\omega_p/\sqrt{2}),p] = 1-\omega_p^2/(\omega_p/\sqrt{2})^2\left[1+\tfrac{3}{5}(k^2+p^2)/k_c^2\right] , \quad (2.17)$$

and use Eq. (2.9), the potential field in $z>0$ is given by integration over p:

$$\int_0^l dz_1 \int_0^\infty dp \frac{1-\epsilon[\vec{k},p(\omega_p/\sqrt{2})]}{\epsilon[\vec{k},p(\omega_p/\sqrt{2})]} \cos(pz_1) \frac{e^{-k|z-z_1|}}{k}$$

$$= -\frac{\pi}{k}e^{-kz} + \frac{\pi}{2}\left(\frac{5}{6}k_c^2+k^2\right)^{-1/2}\left(2e^{-[(5/6)k_c^2+k^2]^{1/2}z} - e^{-kz}\right). \quad (2.18)$$

The first term, $-(\pi/k)e^{-kz}$, diverges at $k=0$ and the second term is negligible compared with the first term in the case $k \ll k_c$. The first term is the potential due to the δ-function-like charge fluctuation, which is easily shown when we neglect the dispersion of $\epsilon(\vec{k},\omega_p/\sqrt{2},p)$ in Eq. (2.16). The second term results from broadening of the charge fluctuation along z direction.

Using the generalized dielectric function[28] for $\epsilon(\vec{k},p,\omega)$ in Eq. (2.16), we can consider not only the momentum-dependent damping frequency for the surface plasmon but also the momentum-independent one. Even in this case, however, we cannot remove the divergence like $1/k$ which appears in the potential field within the linear-response theory, because this divergence essentially results from the pure Coulomb potential, $(2\pi e^2/k)e^{-k|z|}$, from the induced charge fluctuation. As in the high-frequency case, the generalized dielectric constant is nearly equal to the one given in Eq. (2.17) at $k^2+p^2=0$,[29] the first term in Eq. (2.18) is considered to be sufficient for the potential field in the case $k \ll k_c$. Then, using Eqs. (2.16) and (2.1), we obtain the scattering probability due to the surface-plasmon excitation,

$$\sigma_s = \frac{e^2\omega_p}{4\sqrt{2}\pi^2 v}\int d\vec{K}\sum_{\vec{k}} \frac{\hbar\Gamma_s(k)}{[\hbar\omega-\hbar\omega_s(k)]^2+[\hbar\Gamma_s(k)]^2}\frac{1}{k} \times \left|\langle\varphi_{\vec{K}}^{(-)}|\, e^{-k|z|}e^{-i\vec{k}\cdot\vec{x}}\,|\varphi_{\vec{K}}^{(+)}\rangle\right|^2 , \quad (2.19)$$

where $\Gamma_s(k)$ and $\hbar\omega_s(k)$ are the momentum-dependent damping frequency and surface-plasmon excitation energy, respectively.

III. INELASTIC SCATTERING PROBABILITY FOR LOW-ENERGY ELECTRONS

A. Initial and final waves for incident electrons

In LEED we cannot neglect the scatterings by the crystal lattice potential and the absorptions due to the electronic excitation, phonon excitation, etc. So we must consider these effects in the case of calculating the inelastic intensities by using Eqs. (2.15) and (2.19). In order to consider the scattering by the lattice potential, we must use as $\varphi_{\vec{K}}^{(+)}(\vec{r})$ and $\varphi_{\vec{K}'}^{(-)}(\vec{r})$ the wave functions which are solutions of the Schrödinger equation for the system of the incident electron and the crystal potential with the suitable boundary conditions, known as outgoing and incoming conditions, respectively.[30] When the Schrödinger equation contains also a non-Hermitian potential which is due to absorption, it is easily shown that we must use for $\varphi_{\vec{K}}^{(+)}(\vec{r})$ a solution of the Schrödinger equation containing the non-Hermitian potential with the outgoing boundary condition and for $\varphi_{\vec{K}'}^{(-)}(\vec{r})$ a solution of the equation containing its Hermitian-conjugate potential with the incoming boundary condition (see Appendix A). Further, the relation $\varphi_{\vec{K}'}^{(-)*}(\vec{r}) = \varphi_{-\vec{K}'}^{(+)}(\vec{r})$ is shown for the absorptive medium, which is known as the reciprocity law. So we should use the wave function with the outgoing boundary condition like $\varphi_{\vec{K}}^{(+)}(\vec{r})$. As the wave function $\varphi_{\vec{K}}^{(+)}(\vec{r})$ is the one which is used for calculating the elastic intensities in LEED, we can utilize the results derived by several authors.[31,32] Here we use the wave function derived by McRae,[31] which is useful for the isotropic-scatterer version of the electron-core interaction. When we consider that the absorption occurs only inside the crystal (that assumption is used for calculating the elastic intensities) the initial wave function for the incident electron is given by

$z \geq 0$

$$\varphi_{\vec{K}}^{(+)}(\vec{r}) = e^{i(\vec{K}_0 z + \vec{q}\cdot\vec{X})} + \frac{i2\pi f}{A}\sum_{\vec{v}}\sum_{\nu\geq 0}\frac{\exp(i\tilde{K}_\nu|z-z_\nu| - i\,2\pi\nu\vec{v}\cdot\vec{l}_0 + i(\vec{q}+2\pi\vec{v})\cdot\vec{X})}{\tilde{K}_\nu}\varphi^\nu(\nu\vec{l}_0, z_\nu) \quad , \tag{3.1a}$$

$z < 0$

$$\varphi_{\vec{K}}^{(-)}(\vec{r}) = e^{i\vec{K}\cdot\vec{r}} + \frac{i2\pi f}{A}\sum_{\vec{v}} e^{-iK_\nu z}\sum_{\nu\geq 0}\frac{\exp[i\tilde{K}_\nu z_\nu - i\,2\pi\nu\vec{v}\cdot\vec{l}_0 + i(\vec{q}+2\pi\vec{v})\cdot\vec{X}]}{\tilde{K}_\nu}\varphi^\nu(\nu\vec{l}_0, z_\nu) \quad , \tag{3.1b}$$

$$f = \frac{e^{i2\delta_0}-1}{2iK} \quad , \quad \delta_0 = \tfrac{1}{2}\pi \quad , \quad K_\nu = (K^2 - |\vec{q}+2\pi\vec{v}|^2)^{1/2} \quad , \quad \tilde{K}_\nu = (K_\nu^2 + U_0)^{1/2} + i\frac{1}{2\lambda}\left(\frac{K^2+U_0}{K_\nu^2+U_0}\right)^{1/2} \quad . \tag{3.1c}$$

λ is the mean free path which is half of λ_{ee} used by Duke and co-workers,[18,23,24] f is the angle-independent scattering amplitude for an atom and $U_0 = (2m/\hbar^2)V_0$, V_0 being the mean inner potential. $\vec{v}$ is the reciprocal lattice vector parallel to the surface, A is the area of the unit mesh on the subplane parallel to the surface, and $\vec{l}_0$ is the displacement parallel to the surface of a lattice point between a subplane and the next subplane. $z \equiv \nu d$, with ν a positive integer and d the distance between the subplanes. $\varphi^\nu(\nu\vec{l}_0, z_\nu)$ is the effective field on lattice point which exists at $(\nu\vec{l}_0, z_\nu)$. The effective field shows the effect of multiple scattering due to the crystal lattices.

We obtain the final wave function using the reciprocity relation $\varphi_{\vec{K}'}^{(-)*}(\vec{r}) = \varphi_{-\vec{K}'}^{(+)}(\vec{r})$:

$z \geq 0$

$$\varphi_{\vec{K}'}^{(-)*}(\vec{r}) = e^{i\tilde{K}_0' z - i\vec{q}'\cdot\vec{X}} + \frac{i2\pi f'}{A}\sum_{\vec{v}}\sum_{\nu\geq 0}\frac{\exp[i\tilde{K}_\nu'|z-z_\nu| - i2\pi\nu\vec{v}\cdot\vec{l}_0 - (\vec{q}'-2\pi\vec{v})\cdot\vec{X}]}{\tilde{K}_\nu'}\varphi^\nu(\nu\vec{l}_0, z_\nu) \quad , \tag{3.2a}$$

$z < 0$

$$\varphi_{\vec{K}'}^{(-)*}(\vec{r}) = e^{-i\vec{K}'\cdot\vec{r}} + \frac{i2\pi f'}{A}\sum_{\vec{v}} e^{-iK_\nu' z}\sum_{\nu\geq 0}\frac{\exp[i\tilde{K}_\nu' z_\nu - i2\pi\nu\vec{v}\cdot\vec{l}_0 - i(\vec{q}'-2\pi\vec{v})\cdot\vec{X}]}{\tilde{K}_\nu'}\varphi'^\nu(\nu\vec{l}_0, z_\nu) \quad , \tag{3.2b}$$

where the prime means that we take $\vec{K}'$ instead of $\vec{K}$ in Eq. (3.1c).

B. Scattering probability due to the bulk-plasmon excitation

Using Eqs. (2.15), (3.1a), and (3.2a), we obtain the scattering probability due to the bulk-plasmon excitation. Following Duke and Laramore,[18] we keep only two terms in the product of $\varphi_{\vec{K}}^{(+)}(\vec{r})$ and $\varphi_{\vec{K}'}^{(-)}(\vec{r})$. One term is the product of the second term in Eq. (3.1a) and the first term in Eq. (3.2a), known as the amplitude for the diffraction-before-loss process, written D-L process for simplicity. Another term is product of the first term in Eq. (3.1a) and the second term in Eq. (3.2a), known as the amplitude for the loss-before-diffraction process (L-D process). The other terms should be negligible compared with these two terms.[24] Then we obtain

$$\sigma_b = \frac{e^2\omega_p}{4\pi^3 v}\int d\vec{K}'\sum_{\vec{v}}\int_0^{p_c} dp\,\frac{1}{k^2+p^2}\,\frac{\hbar\Gamma_b(k,p)}{[\hbar\omega - \hbar\omega_b(k,p)]^2 + [\hbar\Gamma_b(k,p)]^2}\left[|A_1(\vec{K}',\vec{K}) + A_2(\vec{K}',\vec{K})|^2 - |B_1(\vec{K}',\vec{K}) + B_2(\vec{K}',\vec{K})|^2\right] \quad , \tag{3.3}$$

$$A_1(\vec{K}',\vec{K}) = \left(\frac{1}{k - i\tilde{K}_0' + i\tilde{K}_\nu}[C(\tilde{K}_0', \tilde{K}_0; k) - C(\tilde{K}_\nu, \tilde{K}_0)] - \frac{i}{\tilde{K}_0' - \tilde{K}_\nu + p}C(\tilde{K}_0', \tilde{K}_0; p) - \frac{i}{\tilde{K}_0' - \tilde{K}_\nu - p}C(\tilde{K}_0', \tilde{K}_0; -p)\right.$$
$$\left. + \frac{2i(\tilde{K}_0' - \tilde{K}_\nu)}{(\tilde{K}_0' - \tilde{K}_\nu)^2 - p^2}C(\tilde{K}_\nu, \tilde{K}_0)\right) + \left(\frac{-1}{k - i\tilde{K}_0' - i\tilde{K}_\nu}C(\tilde{K}_0', \tilde{K}_0; k) + \frac{i}{\tilde{K}_0' + \tilde{K}_\nu + p}C(\tilde{K}_0', \tilde{K}_0; p) + \frac{i}{K_0' + K_\nu - p}C(\tilde{K}_0', \tilde{K}_0; -p)\right) \quad , \tag{3.4}$$

$$A_2(\vec{K}',\vec{K}) = \left(\frac{1}{k - i\tilde{K}_0 + i\tilde{K}_\nu'}[C'(\tilde{K}_0, \tilde{K}_0'; k) - C'(\tilde{K}_\nu', \tilde{K}_0')] - \frac{i}{\tilde{K}_0 - \tilde{K}_\nu' + p}C'(\tilde{K}_0, \tilde{K}_0'; p)\right)$$
$$- \frac{i}{\tilde{K}_0 - \tilde{K}_\nu' - p}C'(\tilde{K}_0, \tilde{K}_0'; -p) + \frac{2i(\tilde{K}_0 - \tilde{K}_\nu')}{(\tilde{K}_0 - \tilde{K}_\nu')^2 - p^2}C'(\tilde{K}_\nu', \tilde{K}_0')$$
$$+ \left(\frac{-1}{k - i\tilde{K}_0 - i\tilde{K}_\nu'}C'(\tilde{K}_0, \tilde{K}_0'; k) + \frac{i}{\tilde{K}_0 + \tilde{K}_\nu' + p}C'(\tilde{K}_0, \tilde{K}_0'; p) + \frac{i}{\tilde{K}_0 + \tilde{K}_\nu' - p}C'(\tilde{K}_0, \tilde{K}_0'; -p)\right) \quad , \tag{3.5}$$

$$B_1(\vec{K}',\vec{K}) = \frac{1}{k - i\tilde{K}_0' + i\tilde{K}_\nu}[C(\tilde{K}_\nu, \tilde{K}_0) - C(\tilde{K}_0', \tilde{K}_0; k)] + \frac{1}{k - i\tilde{K}_0' - i\tilde{K}_\nu}C(\tilde{K}_0', \tilde{K}_0; k) \quad , \tag{3.6}$$

$$B_2(\vec{K}',\vec{K}) = \frac{1}{k - i\tilde{K}_0 + i\tilde{K}_\nu}[C'(\tilde{K}_\nu', \tilde{K}_0') - C'(\tilde{K}_0, \tilde{K}_0'; k)] + \frac{1}{k - i\tilde{K}_0 - i\tilde{K}_\nu'}C'(\tilde{K}_0, \tilde{K}_0'; k) \quad , \tag{3.7}$$

where

$$C(\tilde{K}_\nu,\tilde{K}_0)=\frac{i2\pi f}{A\tilde{K}_\nu}\sum_{\nu\geq 0}e^{i\tilde{K}_\nu z_\nu}e^{-i2\pi\nu\vec{v}\cdot\vec{l}_0}\varphi^\nu(\nu\vec{l}_0,z_\nu)\ , \tag{3.8}$$

$$C(\tilde{K}_0',\tilde{K}_0;k)=\frac{i2\pi f}{A\tilde{K}_\nu}\sum_{\nu\geq 0}e^{i\tilde{K}_0' z_\nu}e^{-kz_\nu}e^{-i2\pi\nu\vec{v}\cdot\vec{l}_0}\varphi^\nu(\nu\vec{l}_0,z_\nu)\ , \tag{3.9}$$

$$C(\tilde{K}_0',\tilde{K}_0;\pm p)=\frac{i2\pi f}{A\tilde{K}_\nu}\sum_{\nu\geq 0}e^{i(\tilde{K}_0'\pm p)z_\nu}e^{-i2\pi\nu\vec{v}\cdot\vec{l}_0}\varphi^\nu(\nu\vec{l}_0,z_\nu)\ , \tag{3.10}$$

$$C'(\tilde{K}_\nu',\tilde{K}_0')=\frac{i2\pi f'}{A\tilde{K}_\nu'}\sum_{\nu\geq 0}e^{i\tilde{K}_\nu' z_\nu}e^{-i2\pi\nu\vec{v}\cdot\vec{l}_0}\varphi'^\nu(\nu\vec{l}_0,z_\nu)\ , \tag{3.11}$$

$$C'(\tilde{K}_0,\tilde{K}_0';k)=\frac{i2\pi f'}{A\tilde{K}_\nu'}\sum_{\nu\geq 0}e^{i\tilde{K}_0 z_\nu}e^{-kz_\nu}e^{-i2\pi\nu\vec{v}\cdot\vec{l}_0}\varphi'^\nu(\nu\vec{l}_0,z_\nu)\ , \tag{3.12}$$

$$C'(\tilde{K}_0,\tilde{K}_0';\pm p)=\frac{i2\pi f'}{A\tilde{K}_\nu'}\sum_{\nu\geq 0}e^{i(\tilde{K}_0\pm p)z_\nu}e^{-i2\pi\nu\vec{v}\cdot\vec{l}_0}\varphi'^\nu(\nu\vec{l}_0,z_\nu)\ , \tag{3.13}$$

where $\vec{k}=\vec{q}+2\pi\vec{v}-\vec{q}'$. A_1 and B_1 represent the amplitudes for the D-L process. A_2 and B_2 represent the amplitudes for the L-D process. Equations (3.8) and (3.11) represent the reflection amplitudes for the elastic scattering, from which we obtain the two characteristic peaks in the inelastic intensity versus the incident energy, known as the D-L and L-D peaks. The other amplitudes are peculiar to the inelastic scattering due to the bulk-plasmon excitation.

If we take the kinematical approximation, which means $\varphi^\nu(\nu l_0,z_\nu)\approx e^{i\tilde{K}_0 z_\nu}$ in Eq. (3.10), we obtain the sideband diffraction conditions, $\mathrm{Re}(\tilde{K}_0+\tilde{K}_0'\pm p)d-2\pi\vec{v}\cdot\vec{l}_0=2n\pi$, which were first derived by Duke and Laramore.[18] On the other hand, we obtain resonance conditions $\mathrm{Re}(\tilde{K}_0'-\tilde{K}_\nu)\pm p=0$ and $\mathrm{Re}(\tilde{K}_0-\tilde{K}_\nu')\pm p=0$ from the terms in Eqs. (3.4) and (3.5). These conditions are considered to represent the perpendicular momentum conservation at the inelastic vertex, since these conditions (when $\vec{v}=0$) are obtained in the case of the single-step forward scattering which results from the product of the first terms in Eqs. (3.1a) and (3.2a). The facts which were discussed above are also valid when we take the $\sin(pz)\sin(pz)$-like spectral function used by Duke and co-workers,[18,23,24] instead of the spectral function in Eq. (2.13). It is found from numerical calculations given later that the sideband diffraction conditions contribute to separating clearly the D-L and L-D peaks.

C. Scattering probability due to surface-plasmon excitation

Using Eq. (2.19), (3.1a), (3.1b), (3.2a), and (3.2b), and considering only the D-L and L-D terms, we obtain

$$\sigma_s=\frac{e^2\omega_p}{4\sqrt{2}\pi^2 v}\int d\vec{K}'\sum_{\vec{q}}\frac{\hbar\Gamma_s(k)}{[\hbar\omega-\hbar\omega_s(k)]^2+[\hbar\Gamma_s(k)]^2}\frac{1}{k}\times\left|D_1(\vec{K}',\vec{K})+D_2(\vec{K}',\vec{K})\right|^2\ , \tag{3.14}$$

$$D_1(\vec{K}',\vec{K})=\left(\frac{1}{k+iK_0'-iK_\nu}+\frac{1}{k-i\tilde{K}_0'+i\tilde{K}_\nu}\right)C(\tilde{K}_\nu,\tilde{K}_0)-\left(\frac{1}{k-\tilde{K}_0'+i\tilde{K}_\nu}-\frac{1}{k-i\tilde{K}_0-i\tilde{K}_\nu}\right)C(\tilde{K}_0',\tilde{K}_0;k)\ , \tag{3.15}$$

$$D_2(\vec{K}',\vec{K})=\left(\frac{1}{k+iK_0-iK_\nu'}+\frac{1}{k-i\tilde{K}_0+i\tilde{K}_\nu'}\right)C'(\tilde{K}_\nu',\tilde{K}_0')-\left(\frac{1}{k-i\tilde{K}_0+i\tilde{K}_\nu'}-\frac{1}{k-i\tilde{K}_0-i\tilde{K}_\nu'}\right)C'(\tilde{K}_0,\tilde{K}_0';k)\ , \tag{3.16}$$

where $\vec{k}=\vec{q}+2\pi\vec{v}-\vec{q}'$. $C(\tilde{K}_\nu,\tilde{K}_0)$, $C(\tilde{K}_0',\tilde{K}_0;k)$, etc., are given in Eqs. (3.8)–(3.13). D_1 and D_2 represent the D-L and L-D amplitudes, respectively.

Near the Bragg condition, $\mathrm{Re}(\tilde{K}_0+\tilde{K}_\nu)d-2\pi l_0\cdot v=2n\pi$, the main contribution to the probability is from the first term, $[1/(k+iK_0'-iK_\nu)+1/(k-i\tilde{K}_0'+i\tilde{K}_\nu)]C(\tilde{K}_\nu,\tilde{K}_0)$, in Eq. (3.15). The term $1/(k+iK_0'-iK_\nu)$ is obtained from the field outside the crystal, and plays an important role in the angular profile, because the terms in square brackets are shown nearly proportional to k when we use $K_0'-K_\nu\approx\tilde{K}_0'-\tilde{K}_\nu$ and we obtain a scattering probability nearly proportional to k from Eq. (3.14). Thus, the divergence at $k=0$ appearing in Eq. (3.14) is approximately (not completely) removed near the Bragg condition. This fact is confirmed by the numerical calculations given later.

If we neglect the mean inner potential and the absorption inside the crystal, the scattering probability near the Bragg condition is given by

$$\sigma_s\approx\frac{e^2\omega_p}{\sqrt{2}\pi v}\int d\vec{K}'\sum_{\vec{q}}\frac{\hbar\Gamma_s(k)}{[\hbar\omega-\hbar\omega_s(k)]^2+[\hbar\Gamma_s(k)]^2}\times\frac{k}{[k^2+(K_0'-K_\nu)^2]^2}\left|C(\tilde{K}_\nu,\tilde{K}_0)\right|^2\ . \tag{3.17}$$

This result has the familiar form consisting of the product of the usual surface-plasmon amplitude[33]

and the elastic scattering amplitude.

The terms $C(\vec{K}_0', \vec{K}_0; k)$ and $C'(\vec{K}_0, \vec{K}_0'; k)$ contribute to separating clearly the D-L and L-D peaks. This is confirmed later.

D. Comparision with theory presented by Duke and Laramore

At first we consider the spectral function obtained in this model. In the infinite-square-barrier model it is found from Eq. (2.10c) that the spectral function is not divided completely into parts for the bulk and surface plasmons, in contrast to the hydrodynamic treatment.[26] In the hydrodynamic theory the complete separation of the bulk and surface plasmons essentially results from using a Hermitian operator, which gives only real excitation energy. In the model used here, however we cannot treat the problem by using a Hermitian operator, since we obtain complex energies of the bulk and surface plasmons. Because of this, we cannot utilize the orthogonality and completeness relations,[26] and thus the spectral function is not completely divided into parts for the bulk and surface plasmons. But as the spectral function obtained in this model reduces to the one for the step-density model, where the orthogonality and completeness relations are exactly considered, neglecting dispersion, it is considered to be an approximate result as good as the one used by Duke and co-workers.[18,23,26]

Next we consider the probability due to the surface-plasmon excitation given in Eq. (2.19). Bagchi and Duke[23] used $(k^2+\kappa^2)^{1/2}$, where κ is a cutoff wave number and its magnitude is about 1 Å^{-1}, instead of $1/k$, in order to avoid divergence at $k=0$. But the cutoff wave number used by them is considered too large from a physical point of view, since it is found from the discussion in Sec. II C that the term $1/k$ results from the pure Coulomb interaction from the induced charge fluctuation. The cutoff value to avoid unphysical divergence is considered to be of the order of 10^{-2} Å^{-1}, the inverse of which is about the effective range for the surface-plasmon field.[34]

Finally we consider the relation between the distorted-wave method and the quantum-field-theoretical method. Using the transition matrix $T(\vec{K}', \vec{K})$ for the elastic scattering of the incident electron, we can rewrite Eq. (3.1a) as

$z \geq 0$

$$\varphi_{\vec{K}}^{(+)}(\vec{r}) = e^{i\vec{K}\cdot\vec{r}} + \int e^{i\vec{K}_1\cdot\vec{r}} G_R(\vec{K}_1, E)\, T(\vec{K}_1, \vec{K})\, d\vec{K}_1 \ , \tag{3.18}$$

where $G_R(\vec{K}_1, E)$ is the retarded-electron Green's function. Further, we can rewrite Eq. (3.2a) as

$z \geq 0$

$$\varphi_{\vec{K}'}^{(-)*}(\vec{r}) = e^{-i\vec{K}'\cdot\vec{r}} + \int T(\vec{K}', \vec{K}_1)\, G_R(\vec{K}_1, E')\, e^{-i\vec{K}_1\cdot\vec{r}}\, d\vec{K}_1 \ , \tag{3.19}$$

where we use the reciprocity law and the property that $T(\vec{K}', \vec{K}_1) = T(-\vec{K}_1, -\vec{K}')$.

Before calculating the scattering probability due to the surface plasmon using Eqs. (2.19), (3.18), and (3.19), we assume in Eq. (2.19) that the integration $\int d\vec{r}$ can be replaced by

$$V_c \sum_n \int \delta(\vec{r} - \vec{R}_n)\, d\vec{r} \ , \tag{3.20}$$

where V_c is the unit-cell volume. Using this assumption, when we keep only the term for the D-L process, we obtain

$z \geq 0$

$$\langle \varphi_{\vec{K}'}^{(-)} | \frac{e^{-i\vec{k}\cdot\vec{x}}}{k} | \varphi_{\vec{K}}^{(+)} \rangle = V_c \int d\vec{K}_1\, t(\vec{K}', \vec{K}_1, \vec{k}) \times G_R(K_1, E)\, T(\vec{K}_1, \vec{K}) \ , \tag{3.21}$$

where

$$t(\vec{K}', \vec{K}, \vec{k}) = \sum_n \frac{e^{i(\vec{K}'-\vec{K}_1)\cdot\vec{R}_n}}{k} e^{-kz_n} e^{-i\vec{k}\cdot\vec{R}_n} \ .$$

The amplitude given in Eq. (3.21) is the same as the one derived by Duke and Laramore,[18] and we obtain the same amplitudes for the L-D and D-L-D processes.

It is clear from the above discussion that the results from the distorted-wave method can be identified with the ones from the quantum-field-theoretical method when we use Eqs. (3.18)-(3.20).

E. Model calculations

Here using Eqs. (3.3) and (3.14) we calculate the differential inelastic intensities $d^2\sigma/(d\Omega\, dW)$, where Ω is the solid angle and W the loss energy, from the Al (111) surface. In order to investigate the properties peculiar to inelastic scattering, we take the kinematical approximation for the scattering by the lattice, which means $\varphi^{\nu}(\nu\vec{l}_0, z_\nu) \approx e^{i\vec{K}_0 z_\nu}$ and $\varphi'^{\nu}(\nu\vec{l}_0, z_\nu) \approx e^{i\vec{K}_0' z_\nu}$, and only consider the specular spot $\vec{v}=0$. Following Bagchi and Duke,[23] we take the dispersions of the bulk and surface plasmons as

$$\begin{aligned} \hbar\omega_b(k,p) &= 15.0 + 3.048(k^2+p^2) \ , \\ \hbar\Gamma_b(k,p) &= 0.53 + 0.103(k^2+p^2) + 1.052(k^2+p^2)^2 \ , \end{aligned} \tag{3.22}$$

and

$$\begin{aligned} \hbar\omega_s(k) &= 10.1 + 4.0k + 3.0k^2 \ , \\ \hbar\Gamma_s(k) &= 1.4 + 0.74k \ , \end{aligned} \tag{3.23}$$

and the inner potential $V_0 = 14.7$ eV.

We take $1/k \to (k^2+\kappa^2)^{-1/2}$ in Eq. (3.14) in order to avoid the unphysical divergence, and also $(k^2+p^2)^{-1} \to (k^2+p^2+\kappa^2)^{-1}$ in Eq. (3.3) to compare the bulk-plasmon excitation with the surface-plasmon excitation. We consider two kinds of cutoff wave number, $\kappa = 0.6$ Å^{-1} and $\kappa = 0.65$ Å^{-1}, to see the effects of the cutoff wave number on the inelastic intensity. The former is of the order used by

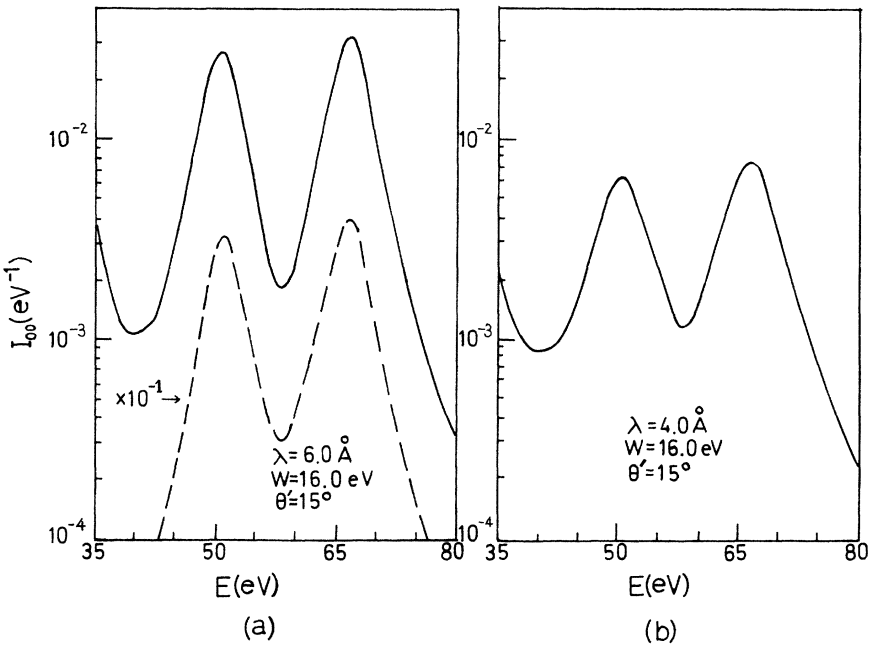

FIG. 1. Kinematical inelastic energy profiles with different mean free paths, for the (00) beam from Al (111). The energy loss W is 16.0 eV. The primary and final polar angles are 15° and the cutoff wave number κ is 0.05 Å^{-1}. (a) Solid curve shows the profile by Eq. (3.3) and dashed curve shows the profile by the spectral function used by Duke and co-workers (Refs. 18, 23, 24), which is multiplied by a factor of 10^{-1}. The mean free path is 6.0 Å. (b) Profile in the case $\lambda = 4.0$ Å.

Duke and co-workers,[23,24] and the latter is of the order of the inverse of the effective range for the surface plasmon. We consider two kinds of mean free path, $\lambda = 4.0$ and 6.0 Å, to see the effects of the absorption on the inelastic intensities. Let (E, θ, ψ) be the energy, polar angle, and azimuthal angle of the incident electron and let $(E - W, \theta', \psi')$ be the same quantities for the scattered electron. We take $\theta = 15°$ and $\psi = \psi' = 0$.

At first we investigate the energy profile, where the scattering angle and loss energy are fixed and only the incident energy is changed. Figure 1(a) shows the energy profiles with the different absorptions for the bulk-plasmon excitation. We obtain the two well-known peaks (D-L and L-D peaks) at $E \approx 50$ and 60 eV, respectively, but we have no peak concerned with the sideband diffraction conditions. Characteristic of the energy profile is the fact that a dip between the two peaks is obtained, which clearly appears in the case of a weak absorption $\lambda = 6$ Å. This dip is considered to result from the sideband diffraction condition, because in the kinematical approximation and the specular reflection case, the energy range for the sideband diffraction condition, $\mathrm{Re}(\vec{K}_0 + \vec{K}_0') \pm p = 2n\pi/d$, exists mainly between the energies of the D-L and L-D peaks.

In order to confirm that this phenomenon is not peculiar to the spectral function given in Eq. (2.13), we show the intensities using the $\sin(pz)\sin(pz')$-like spectral function in Fig. 1(a). We see the same phenomenon in this case. Thus, the sideband diffraction condition contributes to separating clearly the D-L and L-D peaks, and these phenomena are considered to be found in the experimental data given by Burkstrand and Propst.[22] But we must perform dynamical calculations to compare the theoretical results with the experimental results in detail, which are performed when we use the dynamical effective field instead of the kinematical one.

Figures 2(a) and 2(b) show the energy profiles in the case of the surface-plasmon excitation. The D-L and L-D peaks are also obtained and the resonance conditions given by Eqs. (3.9) and (3.12) contribute to separating clearly the two peaks.

Next we investigate the angular profiles where the incident energy and the loss energy are fixed and only the scattering angle is changed. In Figs. 3(a) and 3(b) the angular profiles with the different cutoff wave numbers at the Bragg condition $E \approx 50$ eV are shown to see the effects of the cutoff wave numbers on the profiles. It is clear from these figures that the profile for the surface plasmon is sensitive to the cutoff value in comparison with the one for the bulk plasmon. The minimum value near $\theta' \approx 17°$ is especially sensitive to the cutoff value. It is also found that the relative intensity for the surface plasmon to the one for the bulk plasmon depends on the value of the cutoff wave numbers.

The profile for the bulk plasmon is not so changed except that the position of the maximum moves toward the higher-angle side. The intensities calculated using the $\sin(pz)\sin(pz')$-like spectral function are also shown to compare with our results.

Figures 4(a) and 4(b) show the angular profiles for the bulk- and surface-plasmon excitations in the

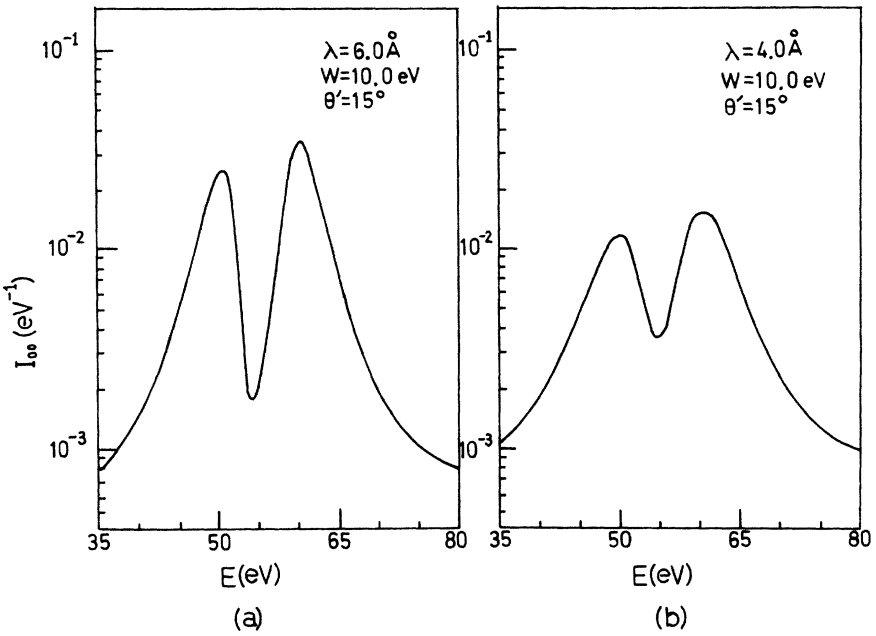

FIG. 2. Kinematical inelastic energy profiles with the different mean free paths for the (00) beam from Al (111). The energy loss W is 10.0 eV. The primary and final polar angles are 15° and the cutoff value κ is 0.05 Å^{-1}. (a) Profile of $\lambda = 6.0$ Å. (b) Profile of $\lambda = 4.0$ Å.

case of $\lambda = 4.0$ Å, which is considered to be suitable for the elastic scattering of LEED. Comparing the profiles in Fig. 4(a) with the ones in Fig. 3(a), it is found that the profiles are barely changed but the intensity for the bulk plasmon relative to the one for the surface plasmon is considerably changed. The decrease of the intensity for the bulk plasmon compared with the one for the surface plasmon in the case of strong absorption shows that the probability of surface-plasmon excitation becomes prominent near the surface.

The angular profiles at the Bragg condition, $E \approx 50$ eV, are qualitatively in agreement with the experimental results by Porteus and Faith,[21] and the relative intensity is also in agreement with the experimental results.

Figure 4(b) shows the angular profiles at the energy where the loss-before-diffraction peak is ex-

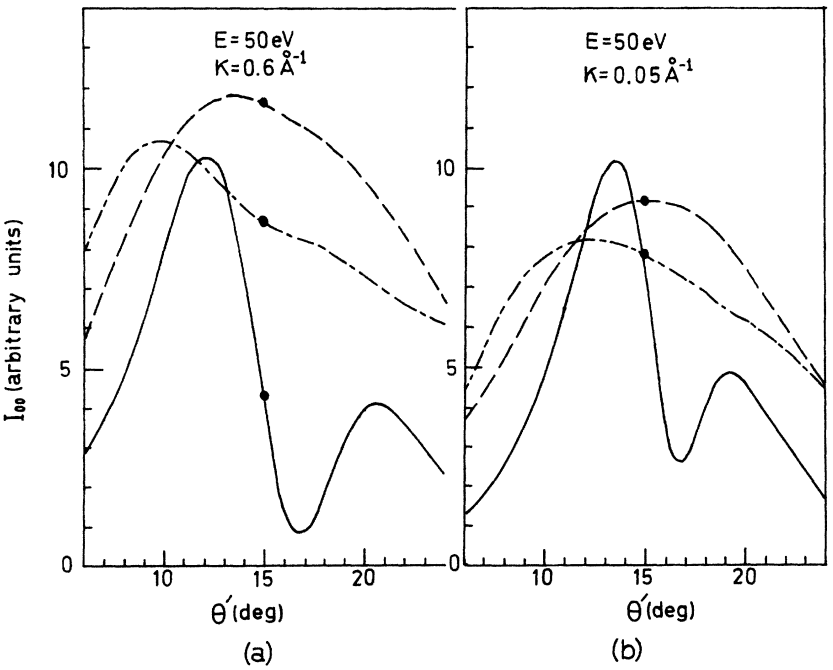

FIG. 3. Angular profiles with different cutoff wave numbers for the (00) beam from Al (111). The primary energy and angle are 50.0 eV and 15° respectively. The mean free path is 6 Å. (a) Cutoff value is 0.6 Å^{-1}. Solid curve shows the profile of $W = 10.0$ eV, and dot-dashed curve and dashed curve show the profile by Eq. (3.3) and the one by the spectral function used by Duke and co-workers, respectively, in the case of $W = 16.0$ eV. (b) Cutoff value is 0.05 Å^{-1}. The intensities are normalized to make the maximum of the profile of $W = 10.0$ coincide with the maximum of $W = 10.0$ in (a). Everything else remains the same as in (a).

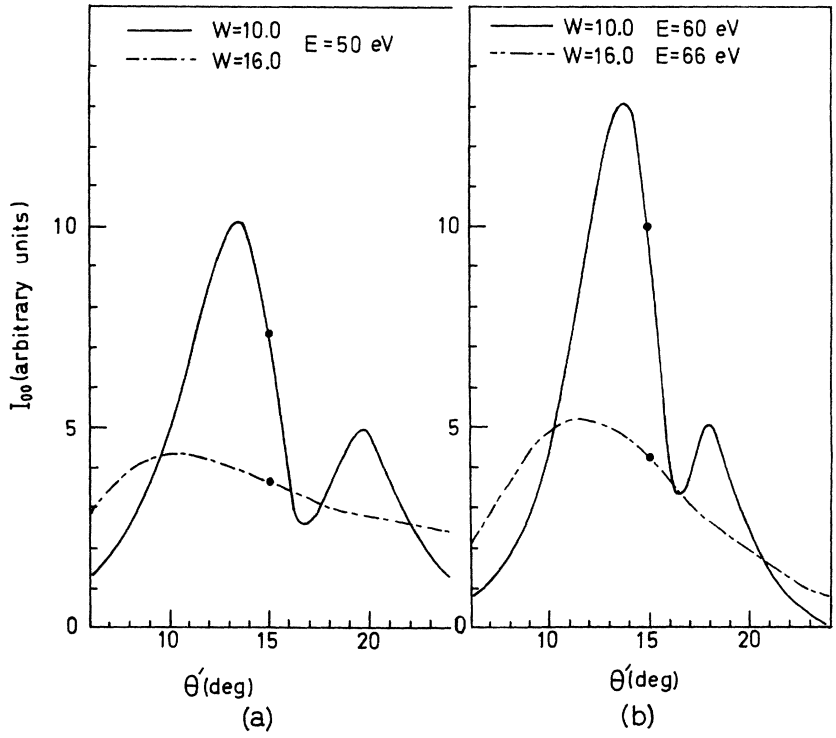

FIG. 4. Angular profiles with different primary energies for the (00) beam from Al (111). The primary angle is 15°. The cutoff value and the mean free path are 0.05 $Å^{-1}$ and 4.0 Å, respectively. The intensities are normalized to make the maximum of the profile of $W=10.0$ and $E=50.0$ eV coincide with the one in Fig. 3 (b). (a) Solid curve shows the profile of $W=10.0$ and $E=50.0$ eV, and dot-dashed curve shows that of $W=16.0$ and $E=50.0$ eV. (b) Solid curve shows the profile of $W=10.0$ and $E=60.0$ eV, and dot-dashed curve shows that of $W=16.0$ and $E=66.0$ eV.

cited. The fact that the intensities at this energy become larger than the intensities at the energy for the Bragg condition is in agreement with the experimental results, but the theoretical curve near $\theta' \approx 16°$ does not represent well the experimental result in which the dip at $\theta' \approx 16°$ does not appear.[21]

IV. RESULTS AND DISCUSSIONS

The scattering probability of the low-energy electron due to the bulk and surface-plasmon excitations has been obtained using the infinite-square-barrier model. This model makes it possible to consider the inelastic scattering of the incident electron by the dissipative medium and has given some insights into the cutoff wave number at $k=0$.

It is also found that the distorted-wave method can be identified with the quantum-field-theoretical method. The distorted-wave method is useful not only for low-energy electrons but also for high-energy electrons. This method is found to be especially useful for investigating the Kikuchi patterns in the Bragg case.[35]

From the energy profiles, it is found that the sideband diffraction conditions obtained here contribute to separating the D-L and L-D peaks clearly and do not make any additional peaks.

From the angular profiles, it is found that the intensity for the bulk plasmon relative to the one for the surface plasmon depends considerably both on the mean free path and on the cutoff wave number. So we must consider the absorption and cutoff value more carefully in detailed comparison with the experimental results.

It is also found that the angular profile for the surface plasmon depends on the cutoff value. On the other hand, it was shown from the discussion in Sec. III C that the scattering amplitude due to the surface-plasmon field outside the crystal plays an important role in the angular profile. This means that we must consider the wave function for the incident electron more carefully, but in our treatment we neglected the effects of the image potential outside the crystal and the nonlocality of the optical potential on the incident wave function, which are not considered to be negligible in LEED. So we must consider more carefully the effects of the cutoff wave number and the incident wave function used on the angular profiles for the surface plasmon, to compare with the experimental results in detail, especially on the profiles at the energy of the L-D peak, because the dip near $\theta' \approx 17°$ does not appear in the experimental results.

We did not present the loss profile because the scattering probability obtained using this model is not completely divided into the bulk-plasmon and surface-plasmon parts, and the results obtained here are considered to be poor approximations in the energy-loss range between the excitation energy of the surface plasmon and that of the bulk plasmon.

ACKNOWLEDGMENTS

The author would like to thank Dr. K. Kambe and Professor Y. H. Ohtsuki for their useful discussions and encouragement.

APPENDIX A

We consider a system which is represented by the Hamiltonian

$$H = H_0 + W + H' \ , \qquad W \equiv V + iU \ , \tag{A1}$$

where H_0 is the Hamiltonian for a noninteracting part, V represents the incident-electron-core interaction, iU represents the absorption, and H' represents the electron-plasmon interaction.

The total wavefunction for the system with the outgoing boundary condition is given (in the following discussions we use the operator form) by

$$|\Psi_a^{(+)}\rangle = |\phi_a\rangle + \frac{1}{E - H_0 + i\epsilon}(W + H')|\Psi_a^{(+)}\rangle \ , \tag{A2}$$

where $|\phi_a\rangle$ represents the initial state for the system. Using Eq. (A2) the transition amplitude is given by

$$T_{ba} = \langle\phi_b|(W + H')|\Psi_a^{(+)}\rangle \ , \tag{A3}$$

where $|\phi_b\rangle$ represents the final state for the system.

The wave function for the Hamiltonian, $H_0 + W$, with the outgoing boundary condition is given by

$$|\chi_a^{(+)}\rangle = |\phi_a\rangle + \frac{1}{E - H_0 + i\epsilon} W |\chi_a^{(+)}\rangle \ , \tag{A4}$$

and the wave function for the Hamiltonian, $H_0 + W^\dagger$, with the incoming boundary condition is given by

$$|\chi_b^{(-)}\rangle = |\phi_b\rangle + \frac{1}{E - H_0 - i\epsilon} W^\dagger |\chi_b^{(-)}\rangle \ , \tag{A5}$$

where $W^\dagger$ represents the Hermitian conjugate operator of W. Substituting $|\phi_b\rangle$, which is obtained from Eq. (A5), into Eq. (A3) and using Eq. (A2), the transition amplitude is rewritten as

$$T_{ba} = \langle\chi_b^{(-)}|H'|\Psi_a^{(+)}\rangle + \langle\chi_b^{(-)}|W|\phi_a\rangle \ . \tag{A6}$$

As the initial state and the final state mean the nonexcited state and the excited state for the plasmon, respectively, the second term in Eq. (A6) vanishes.

$|\Psi_a^{(+)}\rangle$ also satisfies the equation

$$|\Psi_a^{(+)}\rangle = |\chi_a^{(+)}\rangle + \frac{1}{E - H_0 - W + i\epsilon} H' |\Psi_a^{(+)}\rangle \ . \tag{A7}$$

When we keep only the first term in Eq. (A7), the transition amplitude is

$$T_{ba} \approx \langle\chi_b^{(-)}|H'|\chi_a^{(+)}\rangle \ . \tag{A8}$$

Next we investigate the reciprocity law for the absorptive medium. In Eq. (A5) $|\chi_b^{(-)}\rangle$ is represented by the direct product of the plasmon and free-electron states, so that we may consider H_0 as the kinetic energy for the incident electron and $|\phi_b\rangle$ as the plane-wave state which is represented by $e^{i\vec{K}'\cdot\vec{r}}$. If we use the $\vec{r}$ representation, Eq. (A5) becomes

$$\chi_{\vec{K}'}^{(-)}(\vec{r}) = e^{i\vec{K}'\cdot\vec{r}} + \int d\vec{r}' \int d\vec{r}'' \left\langle \vec{r} \left| \frac{1}{E - H_0 - i\epsilon} \right| \vec{r}' \right\rangle \times \langle \vec{r}' | \ W^\dagger \ | \vec{r}'' \rangle \, \chi_{\vec{K}'}^{(-)}(\vec{r}'') \ . \tag{A9}$$

Taking the complex conjugate of Eq. (A9) and using the property $\langle\vec{r}'|W|\vec{r}''\rangle = \langle\vec{r}''|W|\vec{r}'\rangle$, which is generally valid for the optical potential,[36] we obtain

$$\chi_{\vec{K}'}^{(-)*}(\vec{r}) = e^{-i\vec{K}'\cdot\vec{r}} + \int d\vec{r}' \int d\vec{r}'' \left\langle \vec{r} \left| \frac{1}{E - H_0 + i\epsilon} \right| \vec{r}' \right\rangle \times \langle \vec{r}' | \ W \ | \vec{r}'' \rangle \, \chi_{\vec{K}'}^{(-)*}(\vec{r}'') \ . \tag{A10}$$

This equation is the same as the one satisfield by $\chi_{-\vec{K}'}^{(+)}(\vec{r})$, so we obtain the reciprocity relation

$$\chi_{\vec{K}'}^{(-)*}(\vec{r}) = \chi_{-\vec{K}'}^{(+)}(\vec{r}) \ . \tag{A11}$$

APPENDIX B

Here we briefly discuss the spectral function in the high-frequency step-density model. Using the effective potential $V_{\rm eff}(\vec{k}, \omega, z, z')$, the spectral function can be represented by

$$S(\vec{k}, \omega, z, z') = -\,\mathrm{Im} \int dz_1 \int dz_2 \, v(k, z - z_1) \times P_0(\vec{k}, \omega, z_1, z_2) \, V_{\rm eff}(\vec{k}, \omega, z_2, z') \ , \tag{B1}$$

$$S(\vec{k}, \omega, z, z') = -\,\mathrm{Im}[V_{\rm eff}(\vec{k}, \omega, z, z') - v(k, z - z')] \ , \tag{B2}$$

where $V_{\rm eff}(\vec{k}, \omega, z, z')$ satisfies the equation

$$V_{\rm eff}(\vec{k}, \omega, z, z') = v(k, z - z') + \int dz_1 \int dz_2 v(k, z - z_1) \times P_0(\vec{k}, \omega, z_1, z_2) \, V_{\rm eff}(\vec{k}, \omega, z_2, z') \ . \tag{B3}$$

In Eq. (B3), when we take high-frequency limit and suppose that the free-electron density is represented by the step function at the surface, Eq. (B3) can be rewritten as

$0 \le z \le l$

$$V_{\rm eff}(\vec{k}, \omega, z, z') + \frac{\omega_p^2}{2\omega^2} e^{k(z-l)} V_{\rm eff}(\vec{k}, \omega, l, z') + \frac{\omega_p^2}{2\omega^2} e^{-kz} \times V_{\rm eff}(\vec{k}, \omega, 0, z') - \frac{\omega_p^2}{\omega^2} V_{\rm eff}(\vec{k}, \omega, z, z') = \frac{2\pi e^2}{k} e^{-k|z - z'|} \ . \tag{B4}$$

In the other regions of z, we obtain results similar to Eq. (B4). From Eq. (B4) and similar equations, we obtain the effective potential for $z < 0$ and $0 \le z \le 1$,

$z<0$

$$V_{eff}(\vec{k},\omega,z,z')=\frac{2\pi e^2}{k}e^{-k|z-z'|}+\frac{\omega_p^2}{2\omega^2}\frac{2\pi e^2}{k}\left[\left(1-\frac{\omega_p^2}{2\omega^2}\right)e^{kz}e^{-k|z'|}-e^{k(z-l)}e^{-k|z'-l|}+\left(\frac{\omega_p^2}{2\omega^2}\right)e^{k(z-2l)}e^{-k|z'|}\right]\Bigg/$$
$$\left[\left(1-\frac{\omega_p^2}{2\omega^2}\right)^2-\left(\frac{\omega_p^2}{2\omega^2}\right)^2e^{-2kl}\right], \tag{B5}$$

$0\le z\le l$

$$V_{eff}(\vec{k},\omega,z,z')=\frac{2\pi e^2}{k}e^{-k|z-z'|}\Bigg/\left(1-\frac{\omega_p^2}{\omega^2}\right)-\frac{\omega_p^2}{2\omega^2}\frac{2\pi e^2}{k}\left(\frac{1-\omega_p^2/2\omega^2}{1-\omega_p^2/2\omega^2}\right)(e^{-kz}e^{-k|z'|}+e^{k(z-l)}e^{-k|z'-l|})\Bigg/$$
$$\left[\left(1-\frac{\omega_p^2}{2\omega^2}\right)^2-\left(\frac{\omega_p^2}{2\omega^2}\right)^2e^{-2kl}\right]+\left(\frac{\omega_p^2}{2\omega^2}\right)^2\frac{2\pi e^2}{k}\frac{1}{1-\omega_p^2/\omega^2}e^{-kl}(e^{-kz}e^{-k|z'-l|}+e^{k(z-l)}e^{-k|z'|})\Bigg/$$
$$\left[\left(1-\frac{\omega_p^2}{2\omega^2}\right)^2-\left(\frac{\omega_p^2}{2\omega^2}\right)^2e^{-2kl}\right]. \tag{B6}$$

Using Eq. (B2) and the symmetric property of $V_{eff}(\vec{k},\omega,z,z')$ with respect to z and z', we can show from Eqs. (B5) and (B6) that the bulk-plasmon field vanishes outside the crystal. If we notice $\omega=\omega_p$ in Eq. (B6), the spectral function for the bulk plasmon is given by

$$S(\vec{k},\omega,z,z')=-\frac{2\pi e^2}{k}\,\mathrm{Im}\frac{\omega_p^2}{\omega^2-\omega_p^2}[e^{-k|z-z'|}-(e^{-k(z+z')}+e^{k(z+z'-2l)}-e^{-k(z-z'+2l)}-e^{k(z-z'-2l)})/(1-e^{-2kl})]$$
$$\times\theta(z)\,\theta(z')\,\theta(l-z)\theta(l-z'), \tag{B7}$$

when $kl\to\infty$,

$$S(\vec{k},\omega,z,z')=-\frac{2\pi e^2}{k}\,\mathrm{Im}\frac{\omega_p^2}{\omega^2-\omega_p^2}(e^{-k|z-z'|}-e^{-kz}e^{-kz'})\,\theta(z)\theta(z'). \tag{B8}$$

The above results are exactly the same as the spectral function derived by Feibelman *et al.*[26]

On the other hand, the scattering probability given in our previous paper[27] seems to be quite different from the probability derived from Eq. (B8), but when we perform the integration for z in Eq. (2) in the previous paper, we obtain the same result as in Eq. (B8). The difference between the expressions in Eqs. (2) and (B8) results from our having used Eq. (B1) instead of Eq. (B2) to obtain the spectral function.

*Present address: Central Research Laboratory, Hitachi, Ltd., Kokubunji, Tokyo 185, Japan.

[1]J. Thirwell, Proc. Phys. Soc. Lond. 91, 552 (1967).
[2]L. N. Tharp and E. J. Scheibner, J. Appl. Phys. 38, 3320 (1967).
[3]E. Bauer, Z. Phys. 224, 19 (1969).
[4]J. O. Porteus and W. N. Faith, Phys. Rev. B 2, 1532 (1970).
[5]M. P. Seah, Surface Sci. 24, 357 (1971).
[6]P. A. Fedders, Phys. Rev. 153, 438 (1967).
[7]P. J. Feibelman, Phys. Rev. 176, 551 (1968).
[8]A. J. Bennett, Phys. Rev. B 1, 203 (1970).
[9]D. M. Newns, Phys. Rev. B 1, 3304 (1970).
[10]V. Peuckert, Z. Phys. 241, A1 (1971).
[11]J. Harris, Phys. Rev. B 4, 1022 (1971).
[12]D. E. Beck, Phys. Rev. B 4 1555 (1971).
[13]Ch. Heger and D. Wagner, Z. Phys. 244, 499 (1971).
[14]D. E. Beck and V. Celli, Phys. Rev. Lett. 28, 1124 (1972).
[15]W. H. Weber and M. B. Webb, Phys. Rev. 177, 1103 (1969).
[16]J. I. Gersten, Phys. Rev. 188, 774 (1969).
[17]Y. H. Ohtsuki, J. Phys. Soc. Japan 29, 398 (1970).
[18]C. B. Duke and G. E. Laramore, Phys. Rev. B 3, 3183 (1971); G. E. Laramore and C. B. Duke, Phys. Rev. B 3, 3198 (1971); C. B. Duke, G. E. Laramore, and V. Metze, Solid State Commun. 8, 1189 (1970).
[19]A. Bagchi, C. B. Duke, P. J. Feibelman, and J. O. Porteus, Phys. Rev. Lett. 27, 998 (1971).
[20]C. B. Duke and A. Bagchi, J. Vac. Sci. Technol. 9, 738 (1972).
[21]J. O. Porteus and W. N. Faith, J. Vac. Sci. Technol. 9, 1062 (1972).
[22]J. M. Burkstrand and F. M. Propst, J. Vac. Sci. Technol. 9, 731 (1972).
[23]A. Bagchi and C. B. Duke, Phys. Rev. B 5, 2784 (1972).
[24]C. B. Duke and U. Landman, Phys. Rev. B 6, 2956 (1972); Phys. Rev. B 16, 2968 (1972).
[25]C. B. Duke and U. Landman, Phys. Rev. B 7, 1368 (1973).
[26]P. J. Feibelman, C. B. Duke, and A. Bagchi, Phys. Rev. B 5, 2436 (1972).
[27]M. Ichikawa, J. Phys. Soc. Japan 33, 1170 (1972).
[28]S. Adler, Phys. Rev. 126, 413 (1962).
[29]D. Pines, *Elementary Excitations in Solids* (Benjamin, New York, 1964).
[30]T. Wu and T. Ohmura, *Quantum Theory of Scattering* (Prentice-Hall, New York, 1962).
[31]E. G. McRae, J. Chem. Phys. 45, 3258 (1966).
[32]K. Kambe, Z. Naturforsch. 22a, 322 (1967).
[33]E. A. Stern and R. A. Ferrell, Phys. Rev. 106, 874 (1957).
[34]H. Raether, *Springer Tracts in Modern Physics* (Springer Verlag, Berlin, 1965), Vol. 38.
[35]T. Kawamura, M. Ichikawa, and S. Goldsztaub, Phys. Status Solidi (a) 19, 647 (1973).
[36]P. H. Dederichs, in *Solid State Physics*, edited by F. Seitz *et al.* (Academic, New York, 1972), Vol. 27, p. 135.